

## Gas sensitivity of nanostructured coatings based on zinc oxide nanorods under combined activation

© A.A. Ryabko,<sup>1</sup> A.A. Bobkov,<sup>1</sup> S.S. Nalimova,<sup>1</sup> A.I. Maksimov,<sup>1</sup> V.S. Levitskii,<sup>2</sup> V.A. Moshnikov,<sup>1</sup> E.I. Terukov<sup>1,2</sup>

<sup>1</sup> St. Petersburg State Electrotechnical University „LETI“,  
197376 St. Petersburg, Russia

<sup>2</sup> Ioffe Institute,  
194021 St. Petersburg, Russia  
e-mail: a.a.ryabko93@yandex.ru

Received December 14, 2021

Revised January 25, 2022

Accepted January 28, 2022

This paper presents a study of the gas sensitivity of a nanostructured zinc oxide coating to isopropyl alcohol vapor during heating, ultraviolet irradiation, as well as simultaneous heating and irradiation. Simultaneous heating to 150°C and ultraviolet irradiation ensures an increase in the sensor layer response. A 10-fold decrease in the power consumption of an ultraviolet light-emitting diode results in a 1.2-fold decrease in the response of the sensor coating. Reducing the operating temperature of a gas sensor with low power consumption and achieving the required sensitivity can provide adsorption sensors integration into portable devices for monitoring ambient air quality.

**Keywords:** zinc oxide, nanorods, gas sensor, UV irradiation, combined activation.

DOI: 10.21883/TP.2022.05.53683.314-21

### Introduction

Gas sensors serve for the detection of toxic and explosive gases, ambient air quality monitoring, in medical applications, for the control of production processes. Among various types of gas sensors, semiconductor adsorption sensors are usually characterized by low cost, simple design, and high gas analytical response. Due to the mentioned advantages, the use of semiconductor adsorption gas sensors in portable devices for ambient air quality monitoring, namely the detection of nitrogen oxides [1], carbon monoxide [2,3] and other toxic compounds [4], as well as medical supervision of a person's condition in case of diseases by detecting marker volatile organic compounds in exhaled air [5-7].

The response of traditional semiconductor adsorption sensors is based on a change in the resistance of the sensitive layer, which is due to a change in the depletion layer width near the surface of its crystal grains during interaction with gases [8-10]. Various metal oxides [11,12], their compounds and compositions [13,14], impurity-doped metal oxides [15,16] are usually used as sensitive materials. Meanwhile, the morphology of sensitive layers can be very diverse. The sensitive layers can consist of nanoparticles [17-19], nanorods [20,21], nanofibers [22], nanotubes [23], nanoplates [24], various hierarchical structures [25]. As a separate matter, it should be noted the intensive and promising research aimed at using 2D-materials as adsorption gas sensors [26].

The operation of traditional semiconductor adsorption gas sensors is ensured by heating the sensitive layer

to sufficiently high temperatures of 200–400°C [27-30], which increases the power consumption of the sensors and limits their use in portable devices, reduces their safety use for explosive gases. A decrease in the operating temperature of the sensors leads to a rapid decrease in gas sensitivity. Therefore, the opportunity of replacing the heating of the sensitive layer by irradiation has been widely studied recently. For oxide semiconductors, the opportunity of both ultraviolet irradiation with an energy exceeding the forbidden band width [31,32] and irradiation in the visible region of the spectrum [33-35] is being investigated. To use visible radiation, metal oxides are sensitized by doping, decorating with narrower band gap semiconductors or plasmonic nanoparticles. Although the replacement of heating by irradiation ensures the response of the sensor layers to the analyzed gases, irradiation, unlike heating, does not provide desorption of water molecules, and most studies are carried out using synthetic or pre-dried air. Adsorption of water molecules by the sensor layer leads to a decrease and then complete absence of the response to the analyzed gases [36,37]. Therefore, currently, the use of adsorption semiconductor sensors without heating for practical use in an air atmosphere is difficult.

The aim of this paper was to study the opportunity of combined use of heating and ultraviolet (UV) irradiation of a nanostructured zinc oxide layer to reduce the operating temperature of the sensor while providing high gas sensitivity. Lowering the operating temperature should improve the opportunity to integrate adsorption sensors into portable devices for detecting target gases in the ambient atmosphere.

## 1. Experiment

Formation of a gas-sensitive nanostructured zinc oxide layer (Fig. 1) was carried out by an easily scalable two-stage technique based on ultrasonic spray pyrolysis and low-temperature hydrothermal synthesis [38]. Hexamethylenetetramine and zinc nitrate of an equimolar concentration of 25 mM were used as precursors for the hydrothermal synthesis of zinc oxide nanorods. After synthesis, the sample was annealed at a temperature of 500°C for 5 min to remove organic compounds from the surface of the nanostructured ZnO layer.

To confirm the crystal structure, the sample was examined using Raman-scattering spectroscopy (LabRam HR800, Horiba Jobin Yvon) with irradiation of the samples with a solid-state Nd:YAG laser (Torus SLM) with a wavelength of 532 nm (Fig. 2).

For zinc oxide with the wurtzite structure, the active modes are  $E_2(\text{high})$  (438  $\text{cm}^{-1}$ ),  $E_2(\text{low})$  (99  $\text{cm}^{-1}$ ),  $E_2(\text{high})-E_2(\text{low})$  (333  $\text{cm}^{-1}$ ),  $A_1(\text{LO})$  (574  $\text{cm}^{-1}$ ),  $A_1(\text{TO})$  (378  $\text{cm}^{-1}$ ), and  $E_1(\text{LO})$  (590  $\text{cm}^{-1}$ ) and  $E_1(\text{TO})$  (410  $\text{cm}^{-1}$ ) [39]. Figure 2 shows the most intense peaks corresponding to the  $E_2(\text{low})$  and  $E_2(\text{high})$  modes, as well as the peaks corresponding to the  $E_2(\text{high})-E_2(\text{low})$  and  $A_1(\text{LO})$ , which are lower in intensity. The small width and high intensity of the  $E_2(\text{low})$  and  $E_2(\text{high})$  peaks indicate satisfactory crystallinity of the nanorods.

For the sensor layer, the ceramic substrates with interdigital electrodes were used (Sensor Platform, Tesla Blatna) (Fig. 3). The width of the NiCr/Ni/Au electrodes on the substrate and the distance between them was approximately 25  $\mu\text{m}$ . As an irradiation source, a UV LED with a peak wavelength  $\sim 370$  nm was used, which corresponds to the absorption edge of the nanostructured ZnO layer (Fig. 4), with a power of 1 W. The power consumption of the UV LED was monitored by adjustment

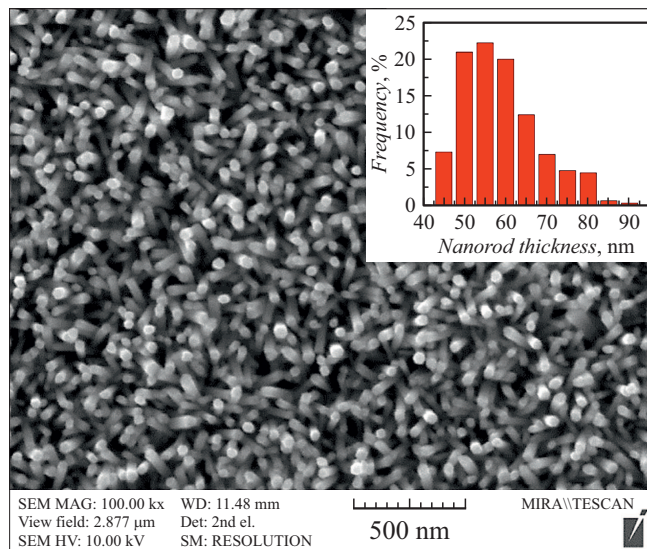


**Figure 1.** SEM image of a nanostructured zinc oxide layer based on nanorods.

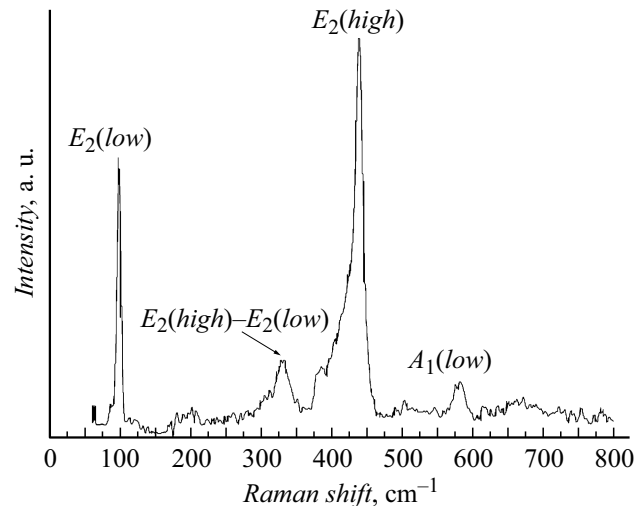


**Figure 2.** Raman spectrum of a nanostructured zinc oxide layer based on nanorods.

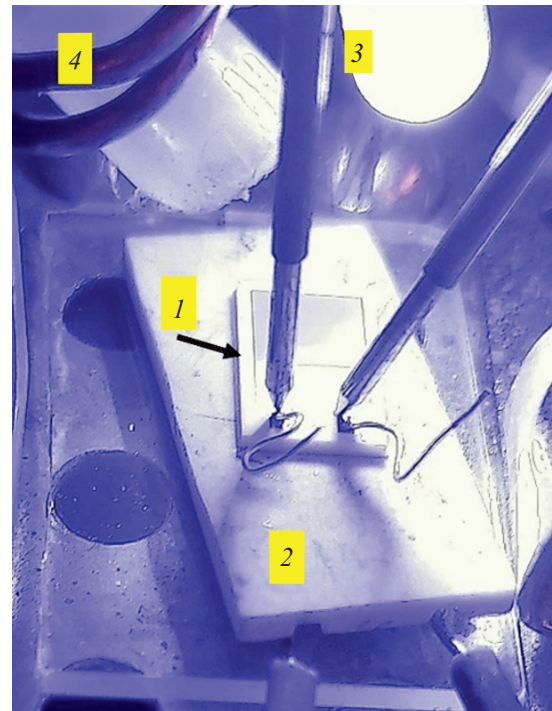


**Figure 3.** Photo of the sample in the sample cell: 1 — ceramic substrate with interdigitated with interdigital electrodes and nanostructured ZnO sensor layer, 2 — heater, 3 — UV LED, 4 — fluoropolymer tube.

of the pulse duty factor of the voltage applied to the UV LED ( $D = \tau/T$ , where  $\tau$  — duration  $T$  — pulse period) with a pulse period value of approximately 2 ms, which is much less than the response time of the sensor layer to UV irradiation.

Isopropyl alcohol vapors were used as the analyzed gas, which acts as a reducing gas, i.e. lead to a decrease in the resistance of the sensor layer based on nanostructured ZnO.

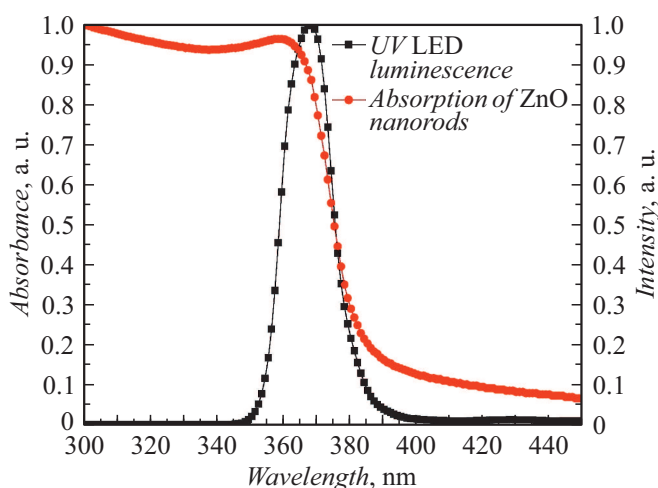


**Figure 4.** Absorption spectrum of nanostructured ZnO layer and luminescence spectrum of UV LED.

Untreated air at a relative humidity of 30–40% was used as a carrier gas. The isopropyl alcohol vapor concentration was specified by mixing the diluent air stream and the isopropyl alcohol vapor stream obtained by passing the air stream through a bubbler tank. The air mixture with isopropyl alcohol vapor was delivered directly to the sample surface through a POM (polyoxymethylene) tube (Fig. 3). The final concentration in the output mixture was determined by the formula

$$C = \frac{P_{\text{gas}} F_{\text{gas}}}{P_{\text{atm}} (F_{\text{gas}} + F_{\text{air}})},$$

where  $P_{\text{gas}}, F_{\text{gas}}$  — is the saturation vapor pressure of the bubbled fluid, the air flow rate through the bubbler tank,  $P_{\text{atm}}$  — atmospheric pressure (taken as 760 mm Hg),  $F_{\text{air}}$  — diluent air flow rate.

Saturation vapor pressure is calculated by the Antoine equation

$$P_{\text{gas}} = 10^{A - \frac{B}{C+T}},$$

where  $A, B, C$  — approximation table parameters,  $T$  — fluid temperature.

Therefore, the isopropyl alcohol vapor concentration was varied by adjusting the air flow through the isopropyl alcohol bubbler tank while maintaining the diluent air flow.

The response of the samples to isopropyl alcohol vapor was evaluated by the formula

$$r = \frac{I_{\text{gas}}}{I_{\text{air}}},$$

where  $I_{\text{gas}}$  — current through the sample when exposed to a gas mixture,  $I_{\text{air}}$  — current through the sample when exposed to air without the target gas.

The heating temperature of the ceramic substrate with interdigital electrodes and a ZnO sensor layer in this study was maintained at 150°C, which is approximately two times lower than the standard heating temperatures of sensor layers. The applied voltage to the interdigital electrodes

was 5V. The current through the sample was measured using a Keithley 6485 picoammeter.

## 2. Results and discussion

The gas analytical response of a nanostructured zinc oxide layer under conditions of UV irradiation (370 nm), heating (150°C), as well as combined heating and UV irradiation to isopropyl alcohol vapor with a concentration of 1000 ppm is shown in Fig. 5, *a*. Meanwhile, the response values of the nanostructured ZnO layer were 1.5, 3.5, and 5.5, respectively. Thus, ultraviolet irradiation provides the smallest response of the sample to the target gas, and the combined effect of heating and irradiation provides the greatest response. The study of the gas-analytical response of the nanostructured ZnO layer with varying isopropyl alcohol vapor concentration (Fig. 5, *b*) showed that an increase in the gas-analytical response of the ZnO sensor layer due to additional UV irradiation during heating is retained when exposed to alcohol vapors of different concentration.

Figure 6 shows the adjustment in the current through the sample at serial connection of heating and additional UV irradiation. The sample was stored in an air atmosphere at room temperature before measurement.

As can be seen from Fig. 6, when the heating is turned on (by 14 min), a rapid increase in current is observed, which then decreases, approaching the equilibrium value. The height and width of this peak will depend on the rate and temperature of heating the sample, the temperature and humidity of the air in which the sample was stored and is located. In the process of heating the semiconductor sensor layer, an increase in the concentration of charge carriers occurs, which determines a rapid increase in current. However, an increase in temperature also leads to the desorption of water molecules, as well as the adsorption of oxygen in the form of charged ions  $\text{O}^-$ , which leads to an increase in the thickness of the blocking layer of the surficial region of nanocrystals and, accordingly, an increase in the resistance of the nanostructured sensor coating. Subsequent additional UV irradiation leads to the second peak  $I(t)$ . The increase in current is associated with additional photogenerated charge carriers, which should also lead to the adsorption of additional oxygen ions. In addition, the predominant form of adsorbed ions can adjust from  $\text{O}^-$  to  $\text{O}^{2-}$ . Thus, the conductivity of the sample decreases and tends to a new stationary value. It should be noted that no  $I(t)$  peak is observed under UV irradiation without heating, which is explained by the presence of adsorbed moisture on the surface of the ZnO [35] sensor layer.

Thus, additional UV irradiation (370 nm) of the nanostructured ZnO layer leads to an increase in the gas analytical response at reduced (up to 150°C) operating temperatures. Heating of the gas-sensitive layer, in addition to the generation of charge carriers, ensures the desorption of water molecules, and UV irradiation provides the generation

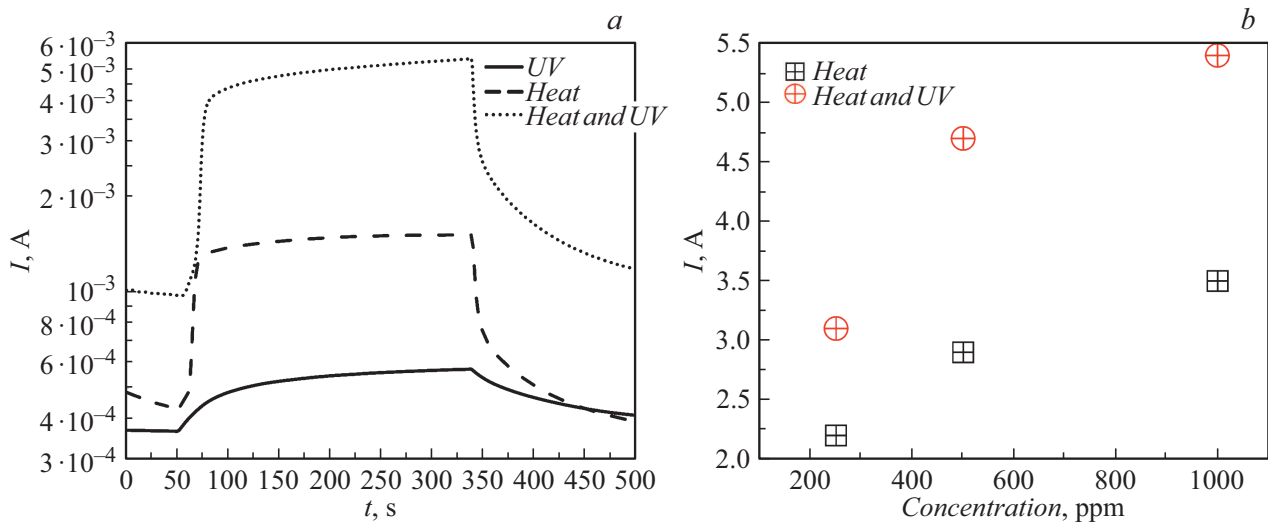


**Figure 5.** Study of the gas-analytical response of a nanostructured layer based on ZnO nanorods: *a* — response of a ZnO layer to 1000 ppm of isopropyl alcohol vapor under UV irradiation (at room temperature) under heating conditions of 150° C and with combined exposure to UV irradiation and heating; *b* — response values under heating conditions of 150° C and under combined exposure to UV irradiation and heating on various concentrations of isopropyl alcohol vapor.

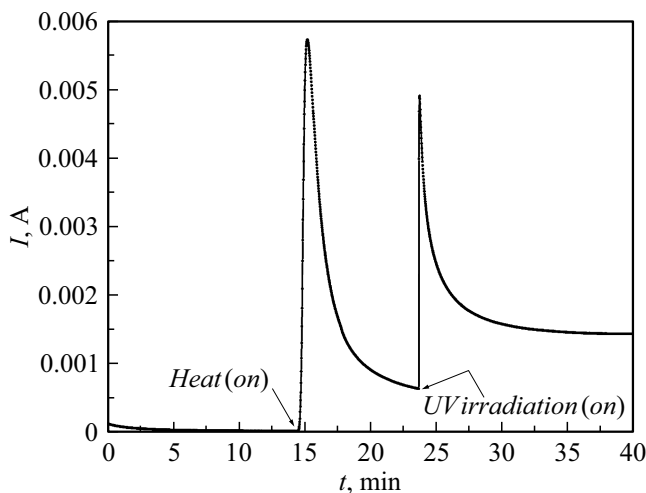


**Figure 6.** Adjustment of the current through the sample of the nanostructured ZnO layer at serial connection of heating and UV irradiation. Voltage applied to the sample — 5 V.

of additional charge carriers. Reducing the operating temperature increases the safety of adsorption sensors for explosive gases, and can also simplify the installation of adsorption sensors inside devices due to the lower heat dissipation power. However, the use of an additional UV LED increases the total power consumption of the sensor.

In this paper, the gas sensitivity of a nanostructured zinc oxide layer was studied under combined heating and UV irradiation of the sensor layer with varying LED power consumption, which was reduced by adjusting the voltage pulse duty factors from 1 to 0.

The gas-sensitive response of the sensor coating under conditions of combined heating and UV irradiation with varying LED power consumption is shown in Fig. 7.

As can be seen from Fig. 7, a decrease in the voltage pulse duty factor of the UV LED supply by 10 times, which corresponds to a power consumption of 100 mW instead of 1 W, leads to a decrease in the response to isopropyl alcohol vapor by only 1.2 times, and a decrease in power consumption by 20 times (up to 50 mW) leads to a decrease in response by 1.3 times. Thus, when using nanostructured ZnO layers, it is possible to use low-power ultraviolet irradiation to operate the sensor in the

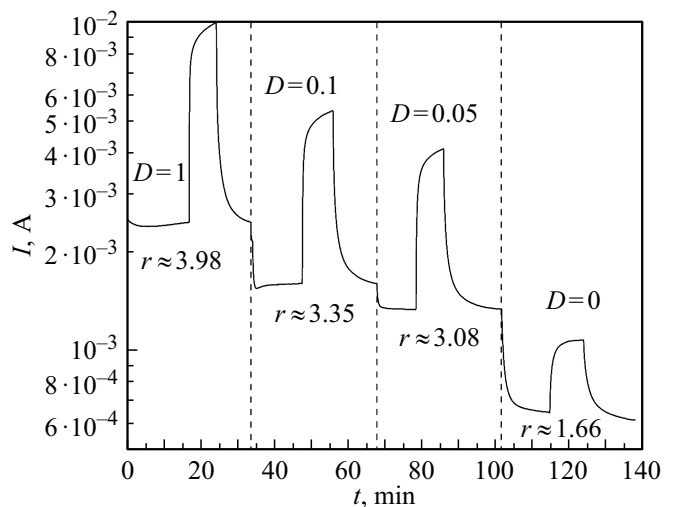


**Figure 7.** Gas-sensitive response of a nanostructured ZnO coating under the combined effect of heating (150° C) and UV irradiation (370 nm) with a decrease in the filling pulse duty factor of the irradiation of the LED supply voltage from 1 to 0.

combined mode of gas sensitivity activation. Therefore, additional UV LED irradiation may not significantly increase the total power consumption of the gas sensor. In addition, the total energy consumption of the sensor at reduced temperatures can be even lower than the energy consumption of many traditional adsorption semiconductor gas sensors ( $\sim 200$  mW). It can be expected that further optimization of the physical and morphological parameters of nanostructured ZnO layers, temperature, and UV irradiation intensity can lead to a significant reduction in the total power consumption while providing the required gas sensitivity.

## Conclusion

This paper presents a study of the gas sensitivity of nanostructured ZnO layers to isopropyl alcohol vapor under heating, UV irradiation, as well as under conditions of combined heating and UV irradiation. It is shown that simultaneous heating and UV irradiation provides an increase in the sensitivity of the sensor coating at reduced operating temperatures. It was found that a decrease in the power consumption of UV irradiation by reducing the voltage pulse duty factor of the LED supply by 10 times leads to a decrease in the gas-sensitive response by a 1.2 times, a decrease in power consumption by 20 times to a decrease in the response by only 1.3 times. The opportunity of using low-intensity UV irradiation and low heating temperatures upon reaching the required sensitivity makes it possible to reduce the power consumption of adsorption sensors based on nanostructured ZnO layers. This, in the aggregate with a decrease in heat removal power, improves the embedding of adsorption gas sensors in portable devices for monitoring the quality of the ambient air.

## Conflict of interest

The authors declare that they have no conflict of interest.

## References

- [1] E.A. Forsh, E.A. Guseva. *Semiconductors*, **54** (2), 217 (2020). DOI: 10.1134/S1063782620020098
- [2] S. Mahajan, S. Jagtap. *Appl. Mater. Today*, **18**, 100483 (2020). DOI: 10.1016/j.apmt.2019.100483
- [3] V.M. Kondratev, A.D. Bolshakov, S.S. Nalimova. *Proceed. 2021 IEEE Conf. Russ. Young Researchers in Electrical and Electronic Engineering (ElConRus)*, 1163 (2021). DOI: 10.1109/ElConRus51938.2021.9396573
- [4] D. Burman, R. Ghosh, S. Santra, S.K. Ray, P. Kumar Guha. *Nanotechnology*, **28**, 435502 (2017). DOI: 10.1088/1361-6528/aa87cd
- [5] N.H. Hanh, L.V. Duy, C.M. Hung, N.V. Duy, Y.-W. Heo, N.V. Hieu, N.D. Hoa. *Sensors and Actuators A*, **302**, 111834 (2020). DOI: 10.1016/j.sna.2020.111834
- [6] G. Katwal, M. Paulose, I.A. Rusakova, J.E. Martinez, O.K. Varghese. *Nano Lett.*, **16**, 3014 (2016). DOI: 10.1021/acs.nanolett.5b05280
- [7] S.J. Kim, S.J. Choi, J.S. Jang, N.H. Kim, M. Hakim, H.L. Tuller, I.D. Kim. *ACS Nano*, **10**, 5891 (2016). DOI: 10.1021/acsnano.6b01196
- [8] S.S. Karpova, V.A. Moshnikov, S.V. Mjakin, E.S. Kolovangina. *Semiconductors*, **47** (3), 392 (2013). DOI: 10.1134/S1063782613030123
- [9] S.S. Karpova, V.A. Moshnikov, A.I. Maksimov, S.V. Mjakin, N.E. Kazantseva. *Semiconductors*, **47** (8), 1026 (2013). DOI: 10.1134/S1063782613080095
- [10] V.A. Moshnikov, S.S. Nalimova, B.I. Seleznev. *Semiconductors*, **48** (11), 1499 (2014). DOI: 10.1134/S1063782614110177
- [11] D. Degler, U. Weimar, N. Barsan. *ACS Sens.*, **4** (9), 2228 (2019). DOI: 10.1021/acssensors.9b00975
- [12] A. Mirzaei, J.-H. Lee, S.M. Majhi, M. Weber, M. Bechelany, H.W. Kim, S.S. Kim. *J. Appl. Phys.*, **126**, 241102 (2019). DOI: 10.1063/1.5118805
- [13] Kh.A. Abdullin, S.K. Zhumagulov, G.A. Ismailova, Zh.K. Kalkozova, V.V. Kudryashov, A.S. Serikkanov. *Tech. Phys.*, **65** (7), 1139 (2020). DOI: 10.1134/S1063784220070026
- [14] C.P. Goyal, D. Goyal, N.S. Ramgir, M. Navaneethan, Y. Hayakawa, C. Muthamizhchelvan, H. Ikeda, S. Ponnusamy. *Phys. Solid State*, **63**, 460 (2021). DOI: 10.1134/S1063783421030070
- [15] R.L. Fomekong, H.M. Tedjieukeng Kamta, J. Ngolui Lambi, D. Lahem, P. Eloy, M. Debliquy, A. Delcorte. *J. Alloys Compounds*, **731**, 1188 (2018). DOI: 10.1016/j.jallcom.2017.10.089
- [16] X. Wang, T. Wang, G. Si, Y. Li, S. Zhang, X. Deng, X. Xu. *Sens. Act. B*, **302**, 127165 (2020). DOI: 10.1016/j.snb.2019.127165
- [17] M.A. Haija, A.F.S. Abu-Hani, N. Hamdan, S. Stephen, A.I. Ayeshe. *J. Alloys Compounds*, **690**, 461 (2017). DOI: 10.1016/j.jallcom.2016.08.174
- [18] I.A. Pronin, N.D. Yakushova, I.A. Averin, A.A. Karmanov, A.S. Komolov, M.M. Sychev, V.A. Moshnikov, E.I. Terukov. *Inorg. Mater.*, **57** (11), 1140 (2021). DOI: 10.1134/S0020168521110108
- [19] I.A. Pronin, N.D. Yakushova, M.M. Sychev, A.S. Komolov, S.V. Myakin, A.A. Karmanov, I.A. Averin, V.A. Moshnikov. *Glass Phys. Chem.*, **44** (5), 464 (2018). DOI: 10.1134/S1087659618050140
- [20] A. Bobkov, V. Moshnikov, A. Varezchnikov, I. Plugin, F.S. Fedorov, V. Goffman, V. Sysoev, V. Trouillet, U. Geckle, M. Sommer. *Sensors*, **19** (19), 4265 (2019). DOI: 10.3390/s19194265
- [21] T.V. Peshkova, D.Ts. Dimitrov, S.S. Nalimova, I.E. Kononova, N.K. Nikolaev, K.I. Papazova, A.S. Bozhinova, V.A. Moshnikov, E.I. Terukov. *Tech. Phys.*, **59** (5), 771 (2014). DOI: 10.1134/S1063784214050259
- [22] G. Korotcenkov. *Nanomaterials*, **11**, 1555 (2021). DOI: 10.3390/nano11061555
- [23] K.-R. Park, H.-B. Cho, J. Lee, Y. Song, W.-B. Kim, Y.-H. Cho. *Sensors and Actuators B: Chemical*, **302**, 127179 (2020). DOI: 10.1016/j.snb.2019.127179
- [24] S.S. Shendage, V.L. Patil, S.A. Vanalakar, S.P. Patil, N.S. Harale, J.L. Bhosale, J.H. Kim, P.S. Patil. *Sensors and Actuators B*, **240**, 426 (2017). DOI: 10.1016/j.snb.2016.08.177

- [25] S. Agarwal, S. Kumar, H. Agrawal, M.G. Moinuddin, M. Kumar, S.K. Sharma, K. Awasthi. *Sensors and Actuators: B. Chemical*, **346**, 130510 (2021). DOI: 10.1016/j.snb.2021.130510
- [26] G.J. Choi, R.K. Mishra, J.S. Gwag. *Mater. Lett.*, **264**, 127385 (2020). DOI: 10.1016/j.matlet.2020.127385
- [27] M.A. Anikina, A.A. Ryabko, S.S. Nalimova, A.I. Maximov. *J. Phys.: Conf. Series*, 012010 (2021). DOI: 10.1088/1742-6596/1851/1/012010
- [28] A.S. Bozhinova, N.V. Kaneva, I.E. Kononova, S.S. Nalimova, Sh.A. Syuleiman, K.I. Papazova, D.Ts. Dimitrov, V.A. Moshnikov, E.I. Terukov. *Semiconductors*, **47** (12), 1636 (2013). DOI: 10.1134/S106378261312004X
- [29] S.S. Nalimova, V.A. Moshnikov, S.V. Myakin. *Glass Phys. Chem.*, **42** (6), 597 (2016). DOI: 10.1134/S1087659616060171
- [30] S.S. Nalimova, I.E. Kononova, V.A. Moshnikov, D.Ts. Dimitrov, N.V. Kaneva, L.K. Krasteva, S.A. Syuleyman, A.S. Bozhinova, K.I. Papazova, A.Ts. Georgieva. *Bulgar. Chem. Commun.*, **49**, 121 (2017).
- [31] G. Li, Z. Sun, D. Zhang, Q. Xu, L. Meng, Y. Qin. *ACS Sens*, **4**, 1577 (2019). DOI: 10.1021/acssensors.9b00259
- [32] A.A. Ryabko, S.S. Nalimova, A.I. Maximov, V.A. Moshnikov. *Proceed. IEEE Conf. Russ. Young Researchers in Electrical and Electronic Engineering (ElConRus)*, 1180 (2021). DOI: 10.1109/ElConRus51938.2021.9396166
- [33] A.S. Chizhov, M.N. Rummyantseva, K.A. Drozdov, I.V. Krylov, M. Batuk, J. Hadermann, D.G. Filatova, N.O. Khmelevsky, V.F. Kozlovsky, L.N. Maltseva, A.M. Gaskov. *Sensors and Actuators: B. Chemical*, **329**, 129035 (2021). DOI: 10.1016/j.snb.2020.129035
- [34] J. Wang, S. Fan, Y. Xia, C. Yang, S. Komarneni. *J. Hazardous Mater.*, **381**, 120919 (2020). DOI: 10.1016/j.jhazmat.2019.120919
- [35] S.S. Nalimova, A.I. Maximov, V.A. Moshnikov, A.A. Bobkov, D.S. Mazing, A.A. Ryabko, E.A. Levkevich, A.A. Semenova. *IEEE Intern. Conf. Electrical Engineering and Photonics (EExPolytech): Proceed.*, 223 (2019). DOI: 10.1109/EExPolytech.2019.8906789
- [36] J. Yang, W. Han, J. Ma, C. Wang, K. Shimanoc, S. Zhang, Y. Sun, P. Cheng, Y. Wang, H. Zhang, G. Lu. *Sensors and Actuators: B. Chemical*, **340**, 129971 (2021). DOI: 10.1016/j.snb.2021.129971
- [37] S.S. Nalimova, A.A. Ryabko, A.I. Maximov, V.A. Moshnikov. *J. Phys.: Conf. Series*, 012128 (2020). DOI: 10.1088/1742-6596/1697/1/012128
- [38] A.A. Ryabko, A.I. Maximov, V.N. Verbitskii, V.S. Levitskii, V.A. Moshnikov, E.I. Terukov. *Semiconductors*, **54** (11), 1496 (2020). DOI: 10.1134/S1063782620110238
- [39] R. Cuscó, E. Alarcón-Lladó, J. Ibáñez, L. Artús, J. Jiménez, B. Wang, M.J. Callahan. *Phys. Rev. B*, **75** (16), 165202 (2007). DOI: 10.1103/PhysRevB.75.165202